Journal of Chemical Health Risks

www.jchr.org

JCHR (2024) 14(6), 1465-1474 | ISSN:2251-6727

Classification of Breast Malignant Tumor Using Ensemble Deep Learning Approach and Magnetic Resonance Imaging

Dr Macha Sarada[1] , Dr Ralla Suresh[2] , Dr. M.Sridevi[3] ,Ravi Kumar R[4], Parvatham Niranjan Kumar[5]

[1]Associate Professor, Department of Computer Science and Engineering, Sri Chaitanaya Institute of Technology & Research(Autonomous), Ponnekal, ,Khammam, Affiliated to JNTUH, Telangana,India.
(https://orcid.org/0000-0003-2910-4623, saradaramaraok@gmail.com)

[2] Associate Professer, HOD, Department of Artificial Intelligence and Data Science, ACE Engineering College(Autonomous),, Medchal Malkajgiri, Telangana, India.
(https://orcid.org/0000-0002-8150-1370 , rella.suresh@gmail.com)

[3] Associate Professor, Dept. of Computer Science and Engineering, CVR College of Engineering(Autonomous), , Hyderabad , Affiliated to JNTUH, Telangana,India
(https://orcid.org/0000-0002-4782-0474 , sreetech99@gmail.com

[4] Assistant Professer, School of Computer Science and Artificial Intelligence, SR University, Warangal, Telangana-506371, India
(https://orcid.org/0000-0001-7775-4079 . ravikumar.racha@gmail.com)

[5] Assistant Professor, CVR College of Engineering, Hyderabad
(https://orcid.org/0000-0002-1383-8078 , niranjan.1216@gmail.com)

(Received: 16 September 2024 Revised: 11 October 2024 Accepted: 04 November 2024)

KEYWORDS
Breast Tumor Classification, Dynamic Contrast-Enhanced Magnetic Resonance Imaging, Multi-Modality Adaptive Feature Fusion Framework, Ensemble Deep Learning, Ultra Sound

ABSTRACT:
Breast cancer stands out as a predominant subject in both biology and health practices, mainly because it remains one of the leading causes of death among women. DCE-MRI and ultrasound together with mammograms, are the most commonly used imaging techniques for breast tumor diagnosis, and each delivers uniquely unique information regarding tumor areas. Even though many algorithms for breast tumor classification exist in the area of machine learning, evaluating multiple modalities separately, it is questionable how their classification performance can be advanced even further. For addressing these challenges, the hybrid deep learning architecture is suggested for the classification of the breast tumor from MRI and US data. First, the input samples are passed through the 2D and 3D convolutional layers for extracting features from each modality separately. Secondly, a discrimination-adaptation module is added to get data features that are independent of the modality by adopting a trio of discriminators through adversarial training. Then, a feature fusion is introduced, using the Multi-Modality Adaptive Feature Fusion (MMAFF) which combines the generic features from each modality and gives more compact features by constructing the affinity matrix and selecting the nearest neighbors only. An integrated MRI-US breast tumor classification dataset comprising 502 cases, including three clinical indicators: Patient data on lymph node metastasis, histological grade, and Ki-67 level is collected to assess the validity of the a priori proposed approach. OUTCOMES: The accuracy is 82%. 5%, 85. 7%, and 89. The detected DPYD variants affected treatment stratification for lymph node metastasis with 6% variance, histological grade, and Ki-67 level clinical indicators.

1. Introduction

Breast cancer remains a severe health concern amongst females since it accounts for a high percentage of cancer-related mortality among women worldwide [1]. Histological examination is particularly favored a great deal since the results generated from this investigation can only be matched by a few diagnostic techniques in terms of sensitivity and specificity in diagnosing breast

Journal of Chemical Health Risks
www.jchr.org
JCHR (2024) 14(6), 1465-1474 | ISSN:2251-6727

cancer [2]. There is significant dependence on histopathology in breast cancer and, therefore, the kind of image that is developed is paramount in enabling accurate pathologic results [3]. Some of the other variables that have been found to significantly impact and influence the accuracy of results of pathology tests include the degree of experience of the clinicians on duty, and the amount of attention deployed by the clinicians in handling samples among others [4]; these inconsistencies are likely to adversely affect the health of a patient in the ward. It is an important aspect that has to do with raising awareness of the disease so that women who are affected can be diagnosed early to help tackle the high mortality rates associated with the disease [5]. Hence, there is the need to incorporate the computer-aided systems because of enhanced computer and artificial intelligence technologies that will help the doctors to provide precise and faster breast cancer treatment [6]. But even in such developments what human expert image analysis offers is a subjective process, time consuming and open to some of the existing challenges such as interpretation bias [7-8].

Deep learning models have further gained more adoption among the computer vision fraternity specifically in biomedical image analysis where it creates a rich feature complement and automatically extract both high and low level features from an image [9-10]. Convolutional neural network, a type of deep learning, is applied to handle histories of histopathological images wherein the primary classifying ranges on two classes [11-12]. CNNs have also been used to learn deep representations from histopathological images, which are used in models built with other classical ML methods for classification of features derived from images [13]. Performance analysis of CNNs as compared to the traditional classifiers in the field of pathology image classification of elite breast cancer images suggests that the former has emerged as the best among them [14]. Breast pathology image analysis through the use of the semi- or fully-automated methods helps pathologists achieve better results, optimize work of the diagnostic process and speed the work up. DL models capitalize on the small features in the images that are hard to be overlooked given their nature [15]. The foremost influences are itemized as tracks;

- The ensemble deep learning method is used for breast tumor classification from MRI and US. The features are extracted from different modalities separately with 2D and 3D convolutional layers.
- A discrimination-adaption module is presented to obtain agnostic-specific features using adversarial learning with three separate discriminators.
- The feature fusion module is proposed by using MAFF to blend the modality-agnostic features and increase the feature compactness by utilizing an affinity matrix with nearest neighbor selection.

The structure of this research is as follows: Section 2 analyzes the literature review, Section 3 expands the proposed method, Section 4 presents the results and discussion, Section 5 presents the current conclusion with future work and finally concludes with references.

2. Objectives

Nouman Ahmad et al. [16] presented the transfer learning (TL) supported multi-resolution breast cancer histopathological image classification. An approach of DL and TL was deduced to classify histopathological images for breast cancer diagnosis. A classification technique for breast histopathological images using TL on a limited training image set was developed to reduce accuracy loss. Initially, whole slide image concatenations were used and CNNs were used for feature extraction. These characteristics were used to select points of discriminant connections, based on which the efficient-net approach was implemented. Whole-slide histopathology image classification was performed using feature extraction derived from an efficient net approach, followed by training a support vector machine (SVM) classifier. Both Efficient-Net and SVM achieved relatively good results, but dependance on TL could produce biases from pre-trained models and datasets that affected the model performance.

Chiagoziem C. Ukwuoma et al. [17] suggested the breast cancer lesion multi-classification using DEEP_Pachi in histopathological images. This research developed DEEP_Pachi to classify breast histopathological images at different amplifications. A developed DEEP-Pachi collected global as well as regional features that were significant for efficient histopathology image classification. The ensemble approach of DenseNet201 and VGG16 was the backbone of the developed model. An approach aimed to extend DEEP-Pachi approach to further disease classifications by histopathological images, such as skin cancer and oral cancer. However,

Journal of Chemical Health Risks

www.jchr.org

JCHR (2024) 14(6), 1465-1474 | ISSN:2251-6727

MLP Block with SGTM neural-like structures was required to replace in this developed approach for assessing the probable best approach.

David Clement et al. [18] developed the histopathological image classification of multi-class breast cancer applying feature representation of multi-scale pooled image (MPIFR) and SVM. A group of four DCNN classes were integrated with SVM classifiers for classifying breast cancer into eight subtype classes, four malignant and benign. A developed approach used power of DCNNs for extracting the most predictive MPIFR from 4 resolutions of BC images, which were then classified by SVM. Eight pre-trained DCNN architectures were trained individually and an ensemble of four best-performing models was used for feature extraction. However, the developed approach does not address the interpretability of the applied DL models that was crucial for understanding the decision-making process in clinical applications.

Muhammad Junaid Umer et al. [19] introduced the multi-class breast cancer classification by 6B-Net with deep feature fusion as well as selection approach. The introduced approach involves three phases; Initially, deep CNN model in 35-layer was presented by a simultaneous processing block. The introduced approach was initially trained by third-party CIFAR-100 dataset for feature learning. This model was further used as a feature extraction tool and then successfully pre-trained the developed model for breast cancer multi-class classification issues. The extracted feature vector was transmitted as input to feature selection of PSO approach and then the feature extraction phase for optimal feature selection. The outputs of introduced 6B-Net model selection vector and ResNet-50 selection vector were sequentially integrated to enhance performance of classification of breast cancer. However, the introduced approach was required to analyze with integration of different feature selection methods for further enhancing the classification accuracy.

Yiping Zhou et al. [20] developed the classification of breast cancer using resolution adaptive network from histopathological images. A new technique of diagnosis was emerging using image processing method and was widely accepted in diagnosis among pathologists. Anomaly Detection with SVM (ADSVM) approach was a SVM based approach for anomaly detection SVM consists of two modules, while Resolution Adaptive Network (RANet) was a resolution network model designed for resolution adaptive. In the ADSVM method, a semi-supervised approach separates misleading and undesirable trained connections to enhance the training performance of RANet model. The Through this data analysis, diagnoses can be made at the patient level and categorized. Also, the procedure can be more efficient depending on patient status classification. However, to enhance classification performance and computational efficiency, a developed approach was required to use a new feature extraction approach that could replicate the features obtained from the RANet model.

Mengyun Qiao et al. [23] developed breast tumor classification based on MRI-US images by disentangling modality features. It employs a discrimination-adaption module to decompose features into modality-agnostic and modality-specific ones, followed by a feature fusion module to enhance the compactness of modality-agnostic features using an affinity matrix with nearest neighbor selection. The method effectively utilizes paired multi-modality information to enhance breast tumor classification performance, providing complementary information from MRI and US images. The method currently focuses on joint predictions based on two modalities, even when data for only one modality is available, which could limit its applicability in certain scenarios.

3. Methods

Specifically, 2D and 3D convolutional layers are first separately applied for the extraction of features from different modalities. Then, a discrimination-adaptation module is designed to learn modality-agnostic features through an adversarial learning process using three different discriminators. Thereafter, a feature fusion module is designed for integration of the modality-agnostic features, which is made more compact using an affinity matrix with nearest neighbor selection. Finally, three different classifier layers are set up for the fused features to obtain the joint prediction of LNM, histological grades, and Ki-67 expression levels.

Journal of Chemical Health Risks
www.jchr.org
JCHR (2024) 14(6), 1465-1474 | ISSN:2251-6727

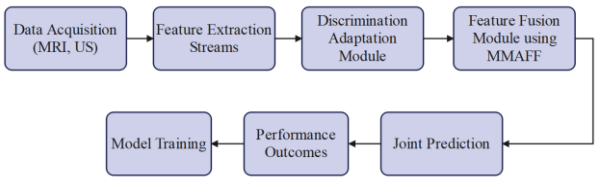

Figure 1 Workflow of the proposed method

3.1. Dataset Acquisition

This approach enrolled 502 patients who received breast ultrasound (US) and magnetic resonance (MR) examinations at Fudan University Shanghai Cancer Center between 2017 and 2020. Institutional review board approval was acquired; however, informed consent was waived for all patients. The inclusion criteria were as follows: (1) visible tumors on preoperative US images and twelve sheets of ultrasound images of each breast tumor; (2) no artifacts of measurements on the US images; (3) preoperative MR images available; (4) primary malignant breast tumors confirmed by core needle biopsy or the pathology of surgery; (5) cases of sentinel lymph node biopsy, axillary lymph node dissection, or fine needle aspiration cytology; (6) no previous treatments before ultrasound and MR examinations, such as neoadjuvant chemotherapy [21,22,23].

For the US examination, all breast images were acquired with a 7-15 MHz linear array transducer using both the Aixplorer US system (SuperSonic Imagine S.A., Aix-en-Provence, France) and the 5-14 MHz linear array transducer using the Resona 5S US system (Shenzhen Mindray Bio-Medical Electronics Co., Ltd., Shenzhen, China). A standardized imaging protocol was utilized: starting from the largest cross-section of the tumor, twelve 2D images were captured with a 180-degree clockwise rotation between each, at equal intervals. The multi-angle images could provide more comprehensive structural information on breast tumors compared with traditional single-view ultrasound images.

MR imaging in the prone position was performed using multiple MR scanners with breast coils, which included a 3-T MR scanner (Skyra; Siemens Medical Solutions, Erlangen, Germany), 1.5-T MR scanner (Signa HDxt; General Electrics, Milwaukee, USA), 3-T MR scanner (Signa HDxt; General Electrics, Milwaukee, USA), and 1.5-T MR scanner (Signa Voyager; General Electrics, Milwaukee, USA). DCE-MRI used gadopentetate meglumine (Gd-DTPA) as the contrast agent administered at a dose of 0.1 mmol/kg. The contrast agent was injected through a pressure syringe intravenously at an injection rate of 1.5-3 mL/s and followed by a 15 mL flush with 0.9% NaCl solution at the same injection rate. All the patients underwent DCE-MRI, which included one pre-contrast image and four post-contrast images for each patient. Clinical features, including LNM level, histological grade, and Ki-67 expression level, were collected from the medical system for all patients. Data dissemination is stated in Table 1.

Table 1 Collection of MRI-US dataset

Indicator	Category	Number
Lymph Node Metastasis	Positive	199
	Negative	303
Histologic Grade	High (3)	202
	Low (1.2)	200
Ki-67 expression level	High	230
	Low	272

3.2. Multiple MRI-US Feature Extraction Streams

A multi-stream feature extractor is used to extract feature embeddings from both modalities. In more detail, we process 12-angle US images and 5-phase DCE-MRI sequences with dissimilar convolutional kernels. Features are extracted by DCEMRI from the left and right breasts with a shared weight network and then concatenated to continue through to the feature discrimination-adaption and fusion steps of the network to reduce network complexity. The feature extractor consists of two modality-specific streams and two modality-agnostic streams, resulting in four sets of features (MRI-agnostic Fa M, MRI-specific Fs M, US-agnostic Fa U, and USspecific Fs U). The stream of each modality is separated in the shallow convolutional layers. The US feature extractor uses a ResNet-50V2 network, which adopts the well-known residual neural network design and has been proven to show superior performance. The DCE-MRI feature extractor uses a 3D ResNet-50V2 structure with 3 × 3 × 3 convolutional kernels, and the features become 512-dimensional after

Journal of Chemical Health Risks
www.jchr.org
JCHR (2024) 14(6), 1465-1474 | ISSN:2251-6727

the last convolutional layer. ResNet-50V2, which uses a large number of layers, skip connections, pretrained weights, and has a high accuracy profile, is a solid choice for use in feature extraction when applied to the classification of tumors in the breast.

3.3. Discrimination-Adaptation Module

A discrimination-adaptation module is adopted, including two modality discrimination modules and one adaptation module, with embedded feature loss and adversarial training strategy. The design guarantees two feature space differences, the modality-specific and the modality-agnostic feature space. The two losses, i.e., LM and LU, are imposed originally through the discrimination modules of the two modalities to achieve feature disentanglement, from one side, to separate the modality-specific features out, and on the other side, to project the modality-specific features to other patients' modality-agnostic features for the same patient. The projection error is formulated as:

$$L_M = E_M\left[\|g_{w_m}(F_M^s) - F_M^a\|\right] (1)$$

$$L_U = E_U\left[\|g_{w_U}(F_U^s) - F_U^a\|\right] (2)$$

where gωM , gωU represents discriminators for modality MRI and US, separately. Similarly, in the discrimination stage, the optimization of gωM, gωU involves the projection of modalityspecific features to corresponding modality-agnostic ones. In the generation stage, to fool the projection, the modality-specific features uncorrelated with modality-agnostic features will be generated by the feature extractors. Such a strategy can make the modality-specific and modality-agnostic feature spaces not related. On the other hand, the feature-extractor can learn specific features different from agnostic features by minimizing and maximizing the projection loss. Then, we utilize modality adaption with three fully connected layers and loss Lmo to remove modality-agnostic features that can be ignored by the modalities:

$$L_{mo} = E_m\left[-\,log\ log\ \left(p\left(y_m|F_m^a, g_{w_a}\right)\right)\right] (3)$$

where gωa represents the parameters of modality adaptation. p(ym|Fa m, gωa) is the predicted probability of the modality agnostic feature Fa m belonging to the ground truth modality ym(ym ∈ US, MRI) based on the model gωa . ym is the one-hot encoded label which is equal to eym ∈ {0, 1}c, corresponding to the ground truth class of modality. The discriminator is trained to predict the image modality while the feature extractors are trained to generate features that cannot be classified. This module ensures that modality-agnostic and modality-specific features are independent and contain less redundant modality information.

3.4. Feature Fusion Module

Next, this approach focus on the specific details of the MMAFF framework in the single-stream state, since different streams are shared under different network structures. The Multi-Modality Adaptive Feature Fusion Framework (MMAFF) processes the input initial skeleton data (X) initially.

3.4.1. Multi-Modality Adaptive Feature Fusion Graph Convolutional Network

In order to produce layer-by-layer predictions of individual streams, the processing results are modified using fully connected layers (FC) and global average grouping (GAP). MMAFF is made up of many STAF (Spatio-Temporal Adaptive Fusion) blocks. Figure 2b depicts the exact structure of STAF. Two modules are included in each STAF block: Temporal Adaptive Feature Fusion (TAFF) and Spatial Attention Graph Convolution (SAGC). The SAGC module is used to dynamically extract the information from spatial dimensions, and the TAFF module is used to adaptively extract temporal relations between joints and fuse multi-scale temporal features with initial features.

3.4.1.1. SAGC Module

This approach adopts to construct a dynamic topology for spatial attention map convolution to dynamically model spatial attention maps. As shown in Figure 2c, this approach simultaneously feed the initial skeleton data into two parallel branches, each of which is processed by a 1 × 1 convolution and a temporal pooling block. By subtracting from the combined outputs of the two branches, attention characteristics are represented. This feature map is summed with the predefined adjacency matrix Ap to obtain the final channel-wise topologies Acwt, i.e., this approach use the attentional feature fusion mechanism to replace the standard residual connection to more effectively combine the data from different temporal and geographical scales.

Journal of Chemical Health Risks
www.jchr.org
JCHR (2024) 14(6), 1465-1474 | ISSN:2251-6727

$$A_{cwt} = \beta Q(X_{in}) + A_p \text{ (4)}$$

where β is a learnable parameter, Ap is the p-th channel shared topology, and Q is the topological relationship of the specific channel, defined as

$$Q(X_i) = \sigma\left(TP\left(\phi(X_{in})\right) - TP\left(\psi(X_{in})\right)\right) \text{ (5)}$$

where σ, φ and ψ are 1 × 1 convolutions, TP is temporal pooling. After this approach obtain the channel-wise topologies Acwt, this approach input the initial skeleton features into a 1 × 1 convolution and multiply the results with Acwt to aggregate the spatial dimension information as follows:

$$X_{out} = A_{cwt} \otimes \left(\theta(X_{in})\right) \text{ (6)}$$

where θ is a 1 × 1 convolution block. ⊗ is matrix multiplication operation.

3.4.1.2. TAFF Module

The temporal adaptive module (TA module) and the temporal feature fusion module (TFF module) make up the multi-scale temporal adaptive feature fusion module. The first section has the ability to dynamically modify the dilation rate and convolution kernel size at various network levels. As shown in Figure 2d, this module is improved on the basis of traditional multi-scale temporal convolution, which contains four branches. To lower the channel dimension, each branch use a 1 × 1 convolution. The adaptive function's two leftmost branches make up its core. Both the dilation rate and the convolution kernel size may be dynamically changed by using a straightforward attention method. The convolution kernel size (ks) and dilation rate (dr) can be dynamically resized according to different dimensions of the output channel. Inspired by the attention mechanism, this approach use the following specific method formula:

$$t = \frac{abs(loglog\ C_{l,2}) + b}{gamma} \text{ (7)}$$

where Cl is l-th network layer output channel dimension, and gamma and b are expressed as the parameters of the mapping function, set to 2 and 1, respectively. At layers 1–4 of the network, ks is 3, and at layers 5–10 of the network, ks is 5. Similarly, dr is 2 at layers 1–7 of the network, and at layers 8–10 of the network, dr is 3. Four branches of different scales obtain X1 through the aggregation function. this approach did not introduce more branches, so there was almost no change in the parameter and computational complexity. For the second part, this approach use an attention feature fusion module to aggregate contextual information of different scales as well as different dimensions along the channel dimension. For the initial feature fusion problem in spatio-temporal modeling, this approach were inspired by TCA-GCN model. Rather, this method uses two input branches, X1 (multi-scale aggregated features) and X (the initial skeleton dat a), to fuse the features of various branches using the AF F module. This approach focus on the information of the initial features and the temporal dimension separately and then perform feature fusion, effectively fusing the initial features and high-dimensional temporal features, resolving the initial feature integration and context aggregation issues and enhancing modeling efficacy.

$$X' = X \otimes M(\cdot) + X_1 \otimes \left(1 - M(\cdot)\right) \text{ (8)}$$

where X denotes the residual connection of the input, and X1 is the concatenated output of multi-scale convolution. The specific formula for M(·)is expressed as

$$Sigmoid\left(L(X \uplus X_1) \oplus G(X \uplus X_1)\right) \text{ (9)}$$

where L(·) and G(·) are the local channel context and global channel context, respectively. The attention module performs first feature fusion on th e input features X and X1, adding local context informat ion to global context information.. After sigmoid activation function, the output value is between 0 and 1. this approach hope to take the weighted average of X and X1 and subtract this group of fusion weights by 1, which can be used as soft selection. The network can learn their individual weights through t raining.

3.5. Joint Prediction

The MRI-specific, US-specific and fused modality-agnostic features are concatenated as the final feature set and fed into three separate classification layers for the joint prediction of LNM, histological grades (HG) and Ki-67 expression levels. A cross-entropy loss is used to train each prediction process. The final task loss combines three losses:

$$L_{cls} = L_{t_1} + L_{t_2} + L_{t_3} \text{ (10)}$$

$$L_{t_1} = E_m\left[-\,log\,log\,\left(p\left(y_{t_1}|[F^a, F_M, F_U], f_{\theta_{t_1}}\right)\right)\right] \text{ (11)}$$

Journal of Chemical Health Risks

www.jchr.org

JCHR (2024) 14(6), 1465-1474 | ISSN:2251-6727

$$L_{t_2} = E_m\left[-\,log\ log\ \left(p\left(y_{t_2}|[F^a, F_M, F_U], f_{\theta_{t_2}}\right)\right)\right] \quad (12)$$

$$L_{t_3} = E_m\left[-\,log\ log\ \left(p\left(y_{t_3}|[F^a, F_M, F_U], f_{\theta_{t_3}}\right)\right)\right] \quad (13)$$

where F_M and F_U represent the features set including modality-agnostic and modality-specific for MRI and US, respectively. t_1 refers the LNM classification task, t_2 refers the HG classification task and t_3 refers the Ki-67 classification task.

3.6. Model Training

The total loss involved the feature loss including the L_M, L_U and L_C for decoupling the features, task loss including the L_{t_1}, L_{t_2}, and L_{t_3} for predicting the three indicators. The min-max strategy is embedded along the network training process and is applied as follows;

$$L_f = L_{cls} + L_c - \lambda_1 L_{mo} - \lambda_2(L_M + L_U) \quad (14)$$

$$L_g = -\lambda_1 L_{mo} - \lambda_2(L_M + L_U) \quad (15)$$

where λ_1 and λ_2 are set to 0.2. The steps include two sub-processes: (1) minimize L_f, which actually maximize the Lmo and the two classification losses L_{fM}, L_{fU}; (2) maximize the L_g in different epochs. g_{ω_N} denotes the parameters of the overall networks except all the other discriminators. The alternative learning process is:

$$f_\theta = arg\ arg\ L_f \quad (16)$$

$$g_{w_a}, g_{w_M}, g_{w_U} = arg\ arg\ L_g \quad (17)$$

4. Results

The DCE-MRI and US images were normalized to [0, 1], augmented and resized to 5 × 256 × 256 × 48 and 12 × 256 × 256, respectively. The two Adam optimizers are used for each loss in 7, a batch size of 6 and epochs of 500 iterations. The training process was stopped if there was no improvement in the loss for 50 consecutive epochs. In addition, the initial learning rate was set to 1 × 10−4 and reduced by a factor of 0.5 if the training loss was no longer improved after 20 epochs. Data augmentation has been widely applied in small and/or imbalanced training sets and shown improvement across many classification tasks. Considering the limited availability of training data, a variety of data augmentation techniques were applied, including mirroring, random scaling, random rotation, gamma correction augmentation and random elastic deformation. We implement the proposed method with PyTorch with a single graphics processing unit (GPU) (NVIDIA Tesla V100 32 GB). The assessment parameter like accuracy, precision, sensitivity, Area Under Curve (AUC) and specificity are taken to estimate model performance. The mathematical formula is given in eq. (18-21),

$$Accuracy = \frac{TP+TN}{TP+FP+TN+FN} \quad (18)$$

$$Precision = \frac{TP}{TP+FP} \quad (19)$$

$$Sensitivity = \frac{TP}{TP+FN} \quad (20)$$

$$Sensitivity = \frac{TN}{TN+FP} \quad (21)$$

True Positive, True Negative, False Positive, and False Negative are represented by the symbols TP, TN, FP, and FN, respectively [24].

4.1. Performance Analysis

The performance evaluation of proposed method is analyzed by collected MRI-US dataset. The ResNet50-v2 layer is used to extract essential features from the data, the MMAFF layer processes the features to analyze temporal relationships in the data. The proposed approach attained the better performance in every indicator such lymph node metastasis, histological grade and Ki-67 level of dataset. Table 1 represents the workflow of the proposed method.

4.2. Comparative Analysis

The proposed model is analyzed comparatively with existing approaches such as MPIFR [18], ADSVM [20] and MUM-Net [21]. The accuracy, precision, sensitivity and specificity are taken as evaluation parameter to estimate model performance. The proposed approach attained the accuracy of 82.5%, 85.7%, and 89.6% from lymph node metastasis, histological grade and Ki-67 level. Table 3 indicates the comparative analysis for proposed method from the existing methods.

Journal of Chemical Health Risks

www.jchr.org

JCHR (2024) 14(6), 1465-1474 | ISSN:2251-6727

Table 2 Performance analysis of the proposed method

Methods	Accuracy (%)	Precision (%)	Sensitivity (%)	Specificity (%)	AUC (%)
Lymph Node Metasis	82.5	82.7	81.9	81.8	85.7
Histo-logical Grade	85.7	5.4	84.8	84.6	87.3
Ki-67 level	89.6	89.7	88.6	88.9	91.2

Table 3 Comparative Analysis of Proposed Method with Various Clinical Indicators

Methods	Methods	Accuracy (%)	Precision (%)	Sensitivity (%)	Specificity (%)	AUC (%)
Lymph Node Metasis	[18]	77.5	77.8	76.9	76.1	79.4
	[20]	79.2	79.1	78.4	78.6	80.8
	[21]	81.4	81.3	80.9	80.5	82.4
	Proposed Method	82.5	82.7	81.9	81.8	85.7
Histological Grade	[18]	79.5	78.4	79.1	79.1	82.6
	[20]	81.5	80.7	81.2	81.5	83.4
	[21]	83.1	82.4	82.6	82.4	84.8
	Proposed Method	85.7	5.4	84.8	84.6	87.3
Ki-67 level	[18]	81.5	81.6	81.4	81.7	81.2
	[20]	82.4	82.9	82.1	82.3	84.1
	[21]	85.4	85.6	84.9	85.4	87.8
	Proposed Method	89.6	89.7	88.6	88.9	91.2

5. Discussion

In MRI images, modality-agnostic features are concentrated in the tumor region inside the breast, which is red in maps of MRI-agnostic features. These modality-specific features are associated with background region information. The view provided by 3D DCEMRI can convey features such as breast symmetry and improve the coverage of 2D US images. In US images, we can observe that modality-agnostic features are mainly focused in the tumor region and that modality-specific features are distinguished from modality-agnostic features. The high-resolution US images of tumors provide detailed information for the inner tumor region and compensate for the relatively limited view of tumors in MRI images.

6. Conclusion

In the proposed approach, the ensemble deep learning method is proposed for breast tumor classification from MRI and US. First, the features are extracted from different modalities separately with 2D and 3D

Journal of Chemical Health Risks

www.jchr.org

JCHR (2024) 14(6), 1465-1474 | ISSN:2251-6727

convolutional layers. Second, discrimination-adaption module is presented to obtain agnostic-specific features using adversarial learning with three separate discriminators. Then, feature fusion module is proposed by using MMAFF to blend the modality-agnostic features and increase the feature compactness by utilizing an affinity matrix with nearest neighbor selection. The integration of MRI-US breast tumor classification dataset is collected that contained 502 cases with the three clinical indicators lymph node metastasis, histological grade and Ki-67 level such as for assessing the developed approach. The experimental results show that MUM-Net achieves state-of-the-art performance and could be applied in further clinical applications in future.

References

1. Zou, Y., Zhang, J., Huang, S. and Liu, B., 2022. Breast cancer histopathological image classification using attention high-order deep network. International Journal of Imaging Systems and Technology, 32(1), pp.266-279.
2. Liu, M., He, Y., Wu, M. and Zeng, C., 2022. Breast histopathological image classification method based on autoencoder and siamese framework. Information, 13(3), p.107.
3. Ahmad, N., Asghar, S. and Gillani, S.A., 2022. Transfer learning-assisted multi-resolution breast cancer histopathological images classification. The Visual Computer, 38(8), pp.2751-2770.
4. Alqahtani, Y., Mandawkar, U., Sharma, A., Hasan, M.N.S., Kulkarni, M.H. and Sugumar, R., 2022. Breast cancer pathological image classification based on the multiscale CNN squeeze model. Computational Intelligence and Neuroscience, 2022.
5. Zhou, Y., Zhang, C. and Gao, S., 2022. Breast cancer classification from histopathological images using resolution adaptive network. IEEE Access, 10, pp.35977-35991.
6. Michael, E., Ma, H., Li, H. and Qi, S., 2022. An optimized framework for breast cancer classification using machine learning. BioMed Research International, 2022.
7. Wakili, M.A., Shehu, H.A., Sharif, M.H., Sharif, M.H.U., Umar, A., Kusetogullari, H., Ince, I.F. and Uyaver, S., 2022. Classification of breast cancer histopathological images using DenseNet and transfer learning. Computational Intelligence and Neuroscience, 2022.
8. Balkenende, L., Teuwen, J. and Mann, R.M., 2022, September. Application of deep learning in breast cancer imaging. In Seminars in Nuclear Medicine (Vol. 52, No. 5, pp. 584-596). WB Saunders.
9. Liu, M., Hu, L., Tang, Y., Wang, C., He, Y., Zeng, C., Lin, K., He, Z. and Huo, W., 2022. A deep learning method for breast cancer classification in the pathology images. IEEE Journal of Biomedical and Health Informatics, 26(10), pp.5025-5032.
10. Rakha, E.A., Tse, G.M. and Quinn, C.M., 2023. An update on the pathological classification of breast cancer. Histopathology, 82(1), pp.5-16.
11. Yu, D., Lin, J., Cao, T., Chen, Y., Li, M. and Zhang, X., 2023. SECS: An effective CNN joint construction strategy for breast cancer histopathological image classification. Journal of King Saud University-Computer and Information Sciences, 35(2), pp.810-820.
12. Jabeen, K., Khan, M.A., Balili, J., Alhaisoni, M., Almujally, N.A., Alrashidi, H., Tariq, U. and Cha, J.H., 2023. BC2NetRF: breast cancer classification from mammogram images using enhanced deep learning features and equilibrium-jaya controlled regula falsi-based features selection. Diagnostics, 13(7), p.1238.
13. Shankar, K., Dutta, A.K., Kumar, S., Joshi, G.P. and Doo, I.C., 2022. Chaotic sparrow search algorithm with deep transfer learning enabled breast cancer classification on histopathological images. Cancers, 14(11), p.2770.
14. Hamedani-KarAzmoudehFar, F., Tavakkoli-Moghaddam, R., Tajally, A.R. and Aria, S.S., 2023. Breast cancer classification by a new approach to assessing deep neural network-based uncertainty quantification methods. Biomedical Signal Processing and Control, 79, p.104057.
15. Rashmi, R., Prasad, K. and Udupa, C.B.K., 2023. Region-based feature enhancement using channel-

Journal of Chemical Health Risks

www.jchr.org

JCHR (2024) 14(6), 1465-1474 | ISSN:2251-6727

wise attention for classification of breast histopathological images. Neural Computing and Applications, 35(8), pp.5839-5854.

16. Ahmad, N., Asghar, S. and Gillani, S.A., 2022. Transfer learning-assisted multi-resolution breast cancer histopathological images classification. The Visual Computer, 38(8), pp.2751-2770.
17. Ukwuoma, C.C., Hossain, M.A., Jackson, J.K., Nneji, G.U., Monday, H.N. and Qin, Z., 2022. Multi-classification of breast cancer lesions in histopathological images using DEEP_Pachi: Multiple self-attention head. Diagnostics, 12(5), p.1152.
18. Clement, D., Agu, E., Suleiman, M.A., Obayemi, J., Adeshina, S. and Soboyejo, W., 2022. Multi-class breast cancer histopathological image classification using multi-scale pooled image feature representation (MPIFR) and one-versus-one support vector machines. Applied Sciences, 13(1), p.156.
19. Umer, M.J., Sharif, M., Kadry, S. and Alharbi, A., 2022. Multi-class classification of breast cancer using 6B-Net with deep feature fusion and selection method. Journal of Personalized Medicine, 12(5), p.683.
20. Zhou, Y., Zhang, C. and Gao, S., 2022. Breast cancer classification from histopathological images using resolution adaptive network. IEEE Access, 10, pp.35977-35991.
21. Qiao, M., Liu, C., Li, Z., Zhou, J., Xiao, Q., Zhou, S., Chang, C., Gu, Y., Guo, Y. and Wang, Y., 2022. Breast tumor classification based on MRI-US images by disentangling modality features. IEEE Journal of Biomedical and Health Informatics, 26(7), pp.3059-3067.
22. Ralla Suresh, Nagaratna Parameshwar Hegde," Intelligent Ensemble Algorithm for Feature Selection and Effective Prediction for Heart Disease Using SVM and KNN. Springer Nature Singapore, International Conference on Information and Management Engineering, Pages 511-517.
23. C. Ravikumar, R. R. Kumar, M. Sarada, M. Sridevi, K. Pabba and M. A. Pasha, "A Comprehensive exploration of machine learning in early detection with a focus on lung and pancreatic cancer for revolutionizing cancer diagnostics," 2024 International Conference on Emerging Technologies in Computer Science for Interdisciplinary Applications (ICETCS), Bengaluru, India, 2024, pp. 1-6.
24. Sarada, Macha, and Ralla Suresh ,2024, Machine Learning-Based Identification and Forecasting of Chronic Illnesses. International Journal of All Research Education and Scientific Methods (IJARESM), 12(6), pp.1293-1304.